

GROUNDING RESISTANCE OF UNIDIRECTIONALLY STIFFENED
DOUBLE HULLS

by

TIMOTHY LEE MCKENNEY

B.S. Naval Architecture and Marine Engineering., Massachusetts Institute of Technology
(1985)SUBMITTED TO THE DEPARTMENT OF
OCEAN ENGINEERING
IN PARTIAL FUFILLMENT OF THE REQUIREMENTS
FOR THE DEGREES OF
NAVAL ENGINEER

and

MASTER OF SCIENCE IN MECHANICAL ENGINEERING

at the

MASSACHUSETTS INSTITUTE OF TECHNOLOGY

June, 1991

© Timothy Lee McKenney, 1991. All rights reserved

The author hereby grants to MIT and the U.S. Government permission to
reproduce and to distribute copies of this thesis document in whole or in part.

Signature of Author.....

Department of Ocean Engineering
May, 1991

Certified by.....

Tomasz Wierzbicki
Thesis Supervisor

Certified by.....

D.M. Parks
Thesis Reader

Accepted by.....

A. Douglas Carmichael, Chairman
Department Committee on Graduate Studies
Department of Ocean Engineering

DISTRIBUTION STATEMENT A

Approved for public release
Distribution Unlimited

92-01508



GROUNDING RESISTANCE OF UNIDIRECTIONALLY STIFFENED DOUBLE HULLS

by

TIMOTHY LEE MCKENNEY

B.S. Naval Architecture and Marine Engineering, Massachusetts Institute of Technology
(1985)

Submitted to the Department of Ocean Engineering in partial fulfillment of the requirements
for the degrees of Naval Engineer and Master of Science in Mechanical Engineering

ABSTRACT

The Oil Pollution Act of 1990, as well as the U.S. Navy's desire for increased survivability, has focused ship structural designers' attention on alternative double hull structures. Unidirectionally Stiffened Double Hulls (USDH) have surfaced as the most promising structural designs due to their producibility. This paper examines the ability of USDH to withstand grounding damage. The extent of hull penetration has been calculated and related to the ship's gross characteristics, hull structure geometry, and the geometry of the obstruction. The extent of hull penetration and lifting for varying reef heights and spreading angles for a USDH tanker is given as an example.



Accession For	
NTIS GRA&I	<input checked="" type="checkbox"/>
DTIC TAB	<input type="checkbox"/>
Unannounced	<input type="checkbox"/>
Justification	
By <i>perform 50</i>	
Distribution/	
Availability Codes	
Dist	Avail and/or Special
<i>A-1</i>	

CONTENTS	
ABSTRACT.....	2
NOMENCLATURE.....	4
INTRODUCTION	5
FORMULATION OF THE PROBLEM.....	1 1
OUTER DYNAMICS OF SHIP GROUNDING	1 3
INITIATION OF LOCAL DAMAGE	1 4
FRACTURE CONTRIBUTION.....	1 9
BENDING CONTRIBUTION.....	1 9
STRETCHING CONTRIBUTION	1 9
TOTAL FORCE DEFORMATION RELATIONSHIP.....	3 0
FORCE BALANCE	3 5
RESULTS AND DISCUSSION	3 7
CONCLUSIONS AND RECOMMENDATIONS.....	3 9
REFERENCES	4 0
APPENDIX A. FABRICATION OF USDH.....	4 1
APPENDIX B. BENDING - MEMBRANE SOLUTION FOR INDENTATION	4 4
APPENDIX C. BENDING CONTRIBUTION	4 7
APPENDIX D. TOTAL FORCE DEFORMATION RELATIONSHIP	4 9
APPENDIX E. FORCE BALANCE.....	5 1

NOMENCLATURE

The following is a list of all of the symbols used in this analysis of damage due to grounding of a USDH ship.

Global parameters of a ship

L_s ; length
 B ; beam
 T ; draft
 s ; distance from bow to point of contact with a rock

Parameters of a reef

Δ_R ; height of a reef above the ship's bottom
 α ; sloping angle of the reef
 β ; spreading angle of the reef

Parameters characterizing the hull girder of a USDH ship

h ; height of cell (separation of double bottom)
 c ; width of cell (separation of longitudinal girders)
 t_{pi} ; thickness of inner hull plating
 t_{pc} ; thickness of outer hull plating
 M_o ; plastic bending moment per unit length
 N_o ; plastic membrane force per unit width

Parameters characterizing material

σ_o ; flow stress
 ϵ_{cr} ; critical strain to rupture (plane strain)

Parameters calculated during analysis

Δ ; vertical penetration depth
 Δ_l ; vertical lift of a ship at the contact point with the reef
 n ; number of cells deformed
 L ; length of transition zone in the longitudinal direction from the moving contact point with the reef to the undamaged part of the ship
 P ; vertical resisting force
 R ; Global reaction force between the rock and the ship

INTRODUCTION

Advanced Double Hull Structures

The U.S. and world maritime communities are realizing a need for environmentally safer tankers. The U.S. Navy is looking to improve affordability and survivability. Container ship operators desire to increase the capacity of Panamax ships. Advanced double hull designs are now being considered as a means of meeting all three of these needs. This chapter will look at an advanced double hull structure and compare it to a conventional mixed frame double hull structure for these three applications.

Conventional, or mixed framed, double hull structures vary considerably with application. Conventional double hull structures are characterized by a grillage of longitudinal stiffeners and transverse frames which support the outer and inner plating. Typically, the inner and outer hulls are joined by deep frames, or partial bulkheads, at short regular intervals. This provides a fairly efficient system of intersecting stiffeners for carrying all structural loads. This structure can be manually fabricated, but is unsuitable for automated fabrication due to frequently intersecting members and short weld lengths.

Two types of advanced double hull structures were considered for this study. The first was a honeycomb mesh between the hulls; this was quickly eliminated due to its inherent fabrication and access problems. The second was the Unidirectionally Stiffened Double Hull (USDH) concept. (Also called Unidirectional Girder System in Reference 1¹, or Advanced Double Hull Design in Reference 2².) A representative cross section segment is depicted in Figure 1. In the USDH structure, longitudinal girders connect the inner and

¹Okamoto, Tomiyasu et al., "Strength Evaluation of Novel Unidirectional-Girder-System Product Oil Carrier by Reliability Analysis" Trans. SNAME, Vol93, 1985.

²Beach, J. "Cluster Technologies," Trans. ASNE Destroyer, Cruiser, and Frigate Symp. 29 Sept. 1990

outer hulls forming generally rectangular cells. These girders stiffen the hull plating and transmit lateral loads to the transverse bulkheads, which are usually double skinned as well. This type of structure can be manually welded but is more suitable for automated fabrication; Appendix A describes some possible fabrication methods.

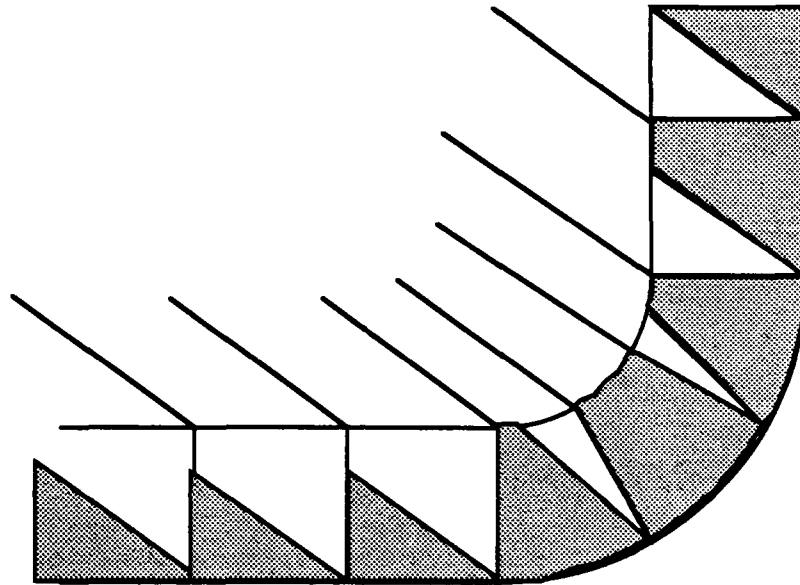


Figure 1 - Segment of Section View of USDH

USDH vs Conventional (Mixed Frame) Double Hull

A USDH structure has some common advantages, regardless of payload, over a conventional double hull in the areas of preliminary design, fabrication, and maintenance. Preliminary ship structural design is in a state of transition from "Design by Rule" to "Design by Analysis". Traditionally ships have been designed largely by rules, dictated by regulatory bodies, based on past experience and empirically derived formulas. This was primarily due to the difficulty of analyzing all the loads applied to a ship and how such a complicated structure would react to them. With the application of computers, design by analysis, or rational design is now possible³. The simplicity of a USDH structure permits a complete strength analysis of the structure. This greatly reduces the uncertainty of the design, allowing applied safety factors to be safely reduced or improving the reliability of the design, this results in reduced cost or improved safety. Also, the number and size of structural discontinuities are reduced, greatly diminishing the number of stress concentrations and potential crack initiation sites.

For ease of fabrication, a USDH structure can be designed with simple and identical components, permitting repetitive marking, cutting, and fitting, operations for ease of automation. The lack of intersecting transverse members enables long continuous welds facilitating mechanized welding by reducing set up time.

Maintenance, in general, for a USDH ship should be easier than conventional double hulls. Access to the cells can be provided through the transverse bulkheads. Once in the cells, personnel are uninhibited by any transverse structure and are supported by the longitudinal girders so that no scaffolding is required. Preservation, repair, and inspection work, can proceed quickly.

³Hughes, Owen F. "Ship Structural Design, A Rationally - Based, Computer - Aided Optimization Approach," SNAME, Jersey City, New Jersey.1988

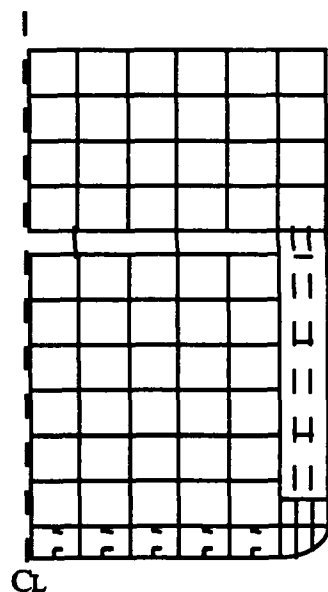
Tankers

In addition to the general advantages listed above; a USDH has a significant operational advantage for tankers. The USDH structure does not require any stiffeners inside the cargo tanks. Structural members internal to the tank on conventional double hull designs complicate tank cleaning and maintenance, and can lead to contamination when changing cargoes in product oil tankers.

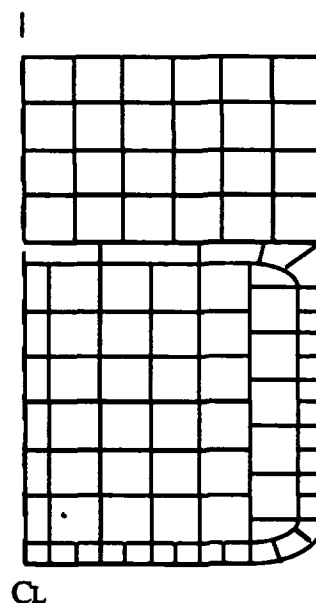
The advantages of a USDH tanker over a conventional single skin tanker are detailed in Reference 1. The principle reason for using a double hull in a tanker is oil spill prevention, the arguments behind this are given in Reference 4.

Containerships

There is a rather unique and untapped advantage for a USDH containership when compared to conventional containership design. A conventional containership has a single hull with a double bottom and large wing tanks - essentially creating a double hull structure. With a USDH structure the wing tanks are replaced with cellular sides. This results in being able to stack an additional column of containers athwartship (11 across) below decks as show in Figure 2. This would result in about a 5% increase in container capacity for the same size ship.



Conventional Structure



USDH Structure

Figure 2 - Containership Midship Hold Cross Sections

Combatant Ships

It is not desirable to estimate the impact of a USDH over a conventional double hull for a combatant ship, since the U.S. Navy combatants are presently single hull ships. The benefits of a USDH design over a conventional single skin combatant design are reviewed in Reference 2. These benefits include greatly improved survivability. Increased structural redundancy should reduce secondary structural damage (damage due to loading of weakened structure) during stranding, grounding, or collision, as well as war time damage. Protection from underwater explosions, and side shell protection should be enhanced by the inherent shock dynamics of double hulls, increased initial contact standoff, and the potential use of between hull fillers. The use of double walled transverse bulkheads should enhance fire isolation due to their inherent insulating properties.

FORMULATION OF THE PROBLEM

In order to derive a method of predicting the grounding performance of Unidirectionally Stiffened Double Hull (USDH) ships a general grounding scenario must be defined. The following scenario is assumed for this analysis. A ship of mass M (displacement full load) runs into a narrow rigid reef. The ship is moving with a forward speed V . The reef contacts the forward end of the ship where the bottom is nearly horizontal (away from the bow), and proceeds directly aft. This contact is assumed to be away from the turn in the bilge and sufficiently inboard so that unsymmetrical moments can be ignored. The height of the reef, Δ_R , is measured above the ships bottom. The sloping angle, α , and spreading angle, β , are measured as shown in Figure 3. These three terms define the shape of the reef. It is assumed that the reef is not crushed during the grounding, therefore Δ_R is constant.

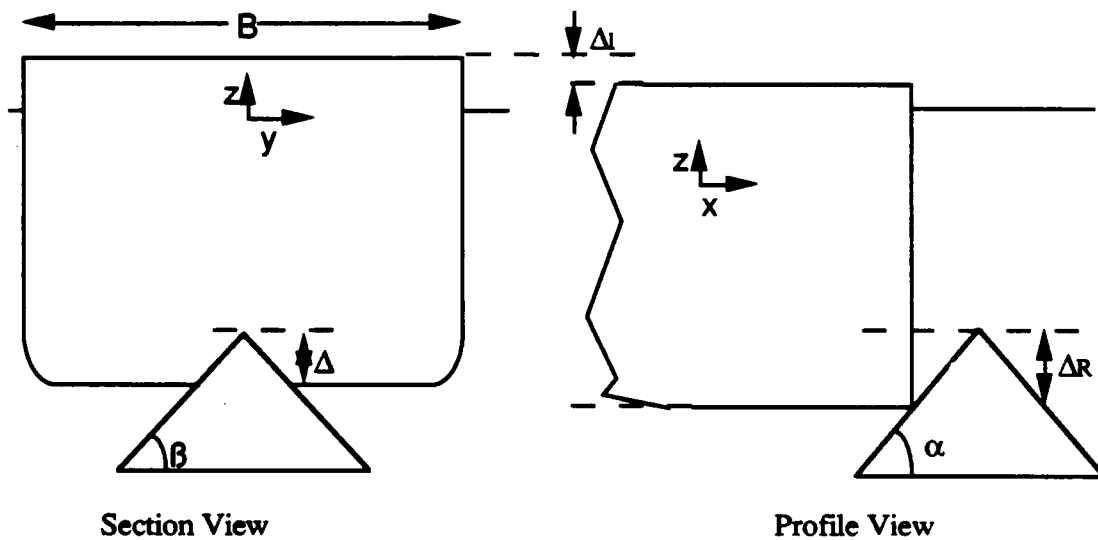


Figure 3 - Ship - Reef Geometry

The problem is then formulated in a similar fashion to that used by Wierzbicki et al, in "Damage Estimates in High Energy Grounding of Ships, June 1990"⁴ for single hull ships. The analysis is broken into four steps.

1. Outer dynamics of the ship grounding
2. Initiation of local damage (penetration).
3. Interaction between overall ship motion and localized damage.
4. Steady-state grounding.

The outer dynamics of a ship grounding is not affected by the structural details of the ship, and are therefore the same for single or double hull ships. The analysis of the outer dynamics of a ship grounding yields an expression for the reaction force as a function of ship dimensions and the height the ship is lifted, Δ_1 .

The initiation of local damage is analyzed by idealizing it as purely vertical damage. The reef is essentially pushed up into the hull to a penetration depth, Δ . The force - deformation characteristics of the double hull, as well as the lateral extent of damage - as a multiple of cell width, C , and longitudinal length, L , of the transition zone between the leading center of damage and the undamaged part of the hull, are determined as a function of this height.

The interaction between the overall ship motion and the localized damage can be resolved as follows. The penetration depth Δ , and the lift Δ_1 , are determined by simultaneously solving the function for the force of deformation, the function for the reaction force from the outer dynamics analysis, and the geometry constraint $\Delta_R = \Delta + \Delta_1$.

This paper will resolve the penetration depth Δ as a function of the hull geometry and the outer dynamics. The steady state phase will be left for subsequent research.

⁴Wierzbicki, T., Rady, E., Peer, D., and Shin, J.G., "Damage Estimates in High Energy Grounding of Ships", Joint M.I.T. - Industry Program on Safe Tankers, Report No.1, June 1990

OUTER DYNAMICS OF SHIP GROUNDING

As previously stated, the outer dynamics of a ship grounding are not affected by the structural details of the ship, and are therefore the same for single or double hull ships.

Appendix A from Reference 5 derives an expression for the reaction force on the ship.

Based on these results, the climbing and descending phase of the ship motion are neglected and the expression for the reaction force is as follows;

$$R = \frac{\rho_w g L_s B \Delta_l}{1 + 12 \left(\frac{1-s}{2 L_s} \right)^2} \quad (1)$$

where 's' is the distance from the bow to the point of impact. This analysis assumes inboard damage and does not address the issue of stability. It is assumed that only a vertical reaction force is generated; any moments are neglected.

INITIATION OF LOCAL DAMAGE

In order to determine the penetration depth of the reef into the hull structure, the initiation of local damage is idealized as purely vertical damage, or stranding. The reef is essentially pushed up into the hull and the force-deformation characteristics, lateral extent of damage, and longitudinal length of the transition zone, are determined as a function of penetration.

This is done by calculating the energy dissipated internally in fracturing, bending, and stretching, of the hull structure. The internal energy dissipation is set equal to the external work, and the function for the force required for deformation is determined. In order to carry out these calculations a realistic mode of deformation / failure for a unidirectionally stiffened double hull over several cells is established. Using stiff paper models of the cellular structure the following failure geometry is established for the cellular hull construction. A square cell, $h=c$, and a moderate β are depicted. Variable h , c , and β , are used in the calculations.

FAILURE GEOMETRY

A reef, of height Δ_R above the baseline of the ship and spreading angle β , is pressed up into the bottom of the hull, as shown in Figure 2.

The reef comes first in contact with the outer plate. A diamond shape deformation zone is assumed as shown in Figure 4.a. The cell width, 'c', is the observed width for the initial plate bending. The length L is later determined using the minimization of membrane and bending energy.

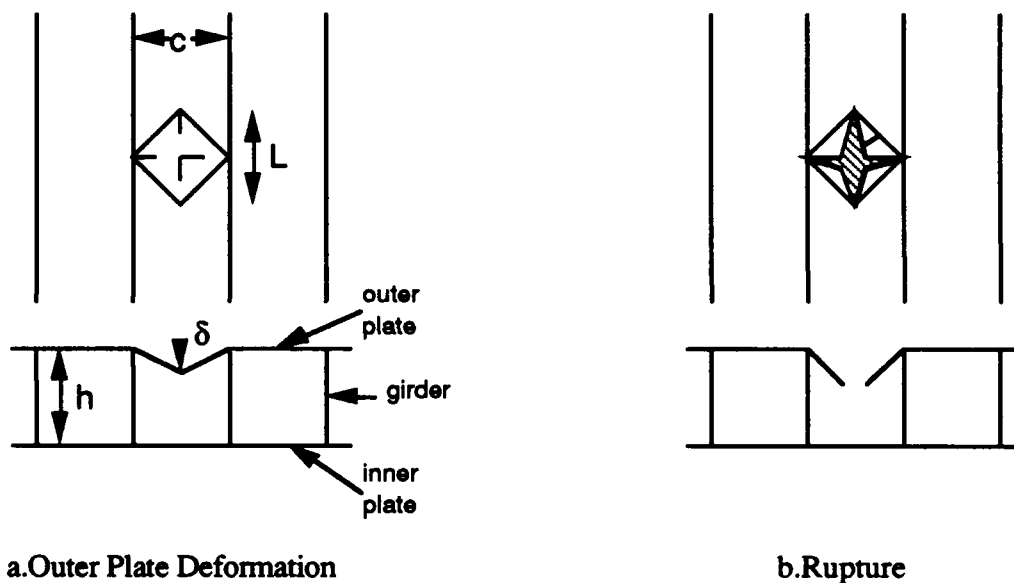


Figure 4 - Diamond Shape Deformation Zone of the Outer Plate

This initial phase continues until the outer plate ruptures or the first set of girders is reached. After the diamond section of plate ruptures, it no longer contributes any membrane energy. The ruptured outer plate is shown in Figure 4.b.

Once the first set of girders are reached by the rock a second phase begins. A second set of hinges in the outer plate are established extending out to the next set of girders as shown in Figure 5.a. The girders are deformed as shown in Figure 5.b.

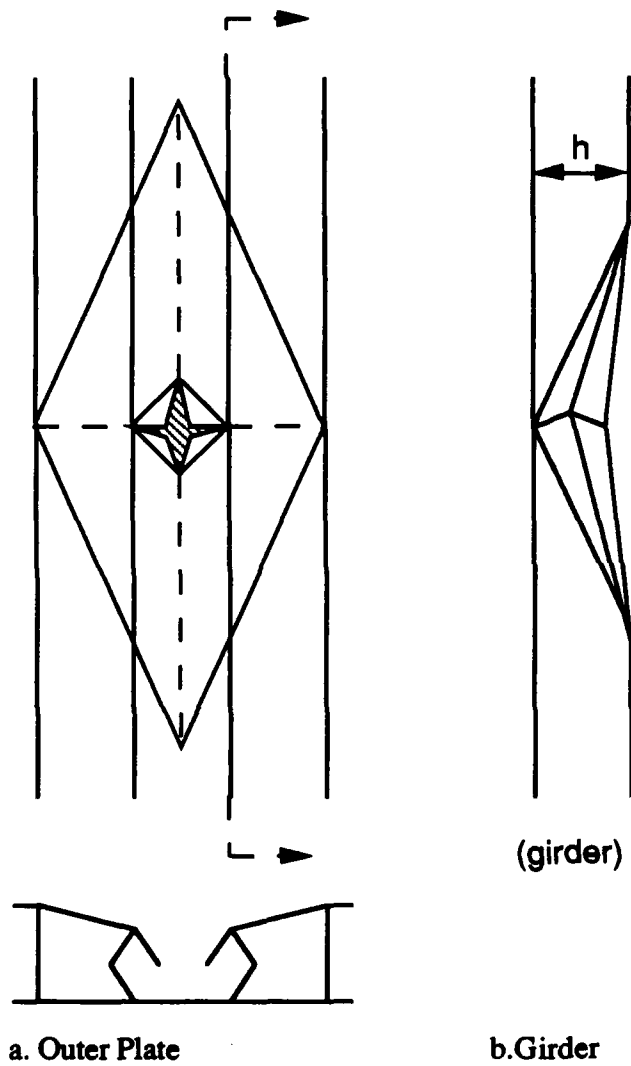


Figure 5 - Second Phase Deformation of Outer Plate and Girders

This phase continues until a second rupture occurs as shown in Figure 6.a, the next set of girders are reached by the sides of the reef, or the inner plate is reached by the apex of the reef as shown in Figure 6.b; depending on β , c , and h .

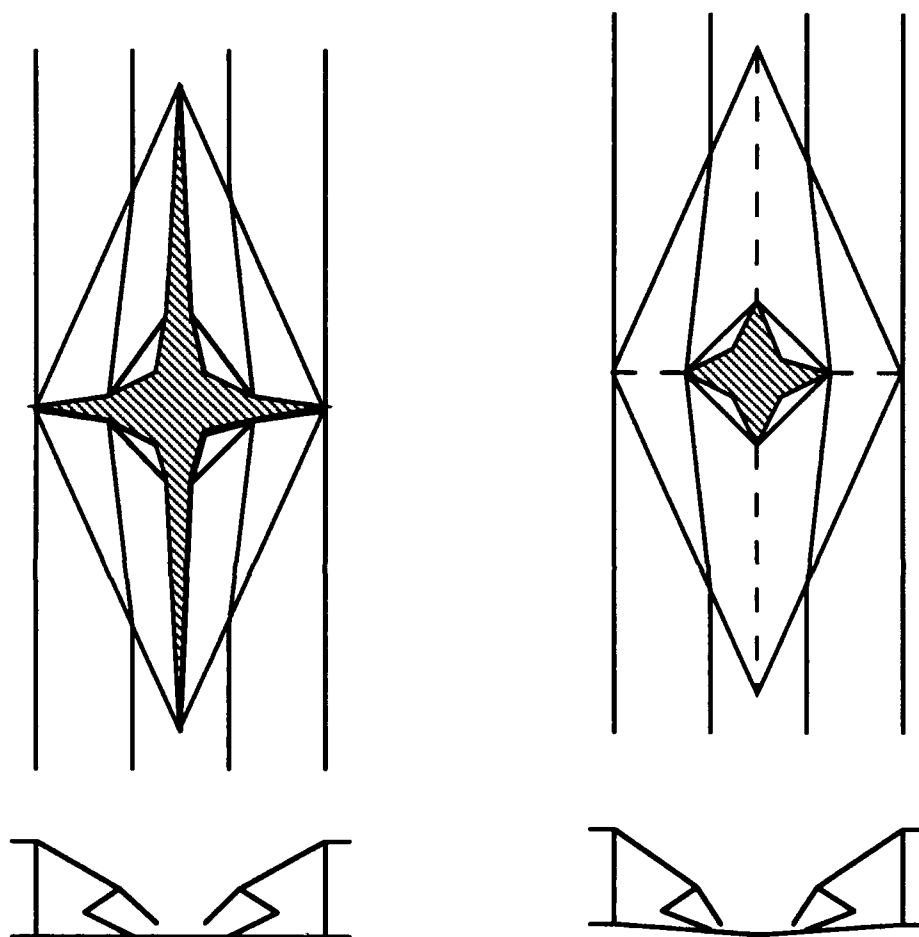


Figure 6.a - Second Rupture of Outer Plate Figure 6.b - Inner Plate Deformation

The inner plate deforms and ruptures in a manner similar to the outer plate, with one exception. For moderate angles β , the rock will already be pressing against the first set of girders when the top of the rock reaches the inner plate. It is observed that this results in the first set of hinges in the outer plate forming a diamond limited by the second girder position. This pattern of the hinge extending out to the next set of undeformed girders

continues as the damage extends laterally over 'n' cells. Figure 7 shows the initial inner plate rupture over three cells.

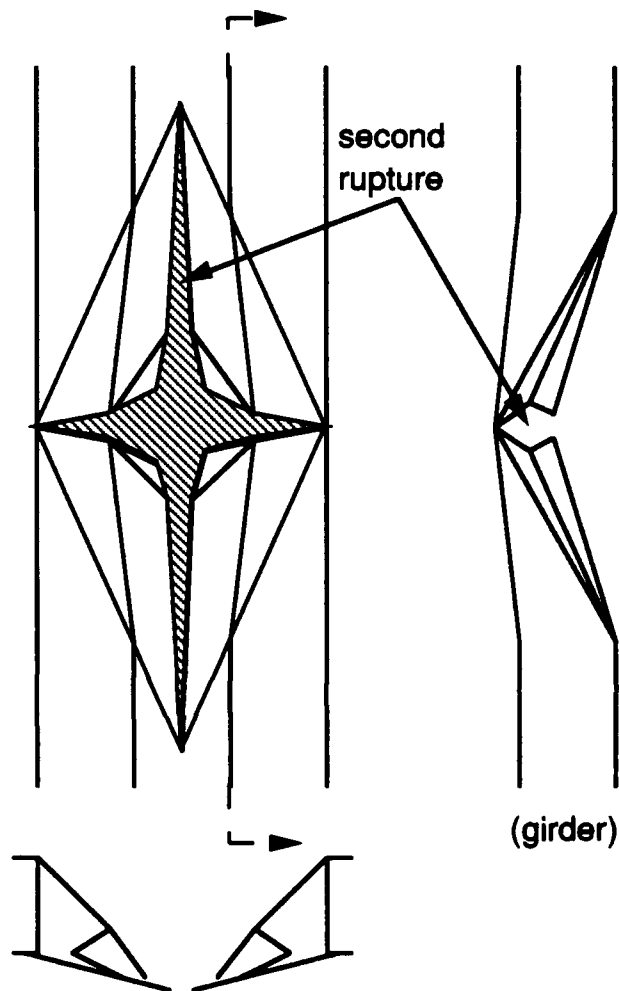


Figure 7 - Inner Plate Rupture Over Three Cells

Minimization of total energy dissipation with penetration depth is used to solve for the longitudinal length of the transition zone, L , for a given lateral extent of damage, nC . These calculations are shown in Appendix B.

FRACTURE CONTRIBUTION

As indicated in Reference 5, the fracturing of the steel is estimated to contribute only about 1% - 2% of the total energy dissipation and is therefore neglected in this analysis.

BENDING CONTRIBUTION

The bending of the steel in a USDH structure is estimated to be between 1.5%-8% (1.5% for simple plate, and 8% for well stiffened plates) of the total energy dissipation. Appendix C derives these percentages for the crushing of one cell using plastic hinge analysis. As the lateral extent of damage is increased beyond one cell, the damaged steel must be re-bent as it is pushed away. The relative bending contribution of the total energy dissipation will therefore increase with the lateral extent of damage. The plating that is already ruptured can no longer be stretched and will not contribute additional membrane energy dissipation. Further analysis is required to determine the amount of energy required for re-bending. For this analysis it is assumed that the increase in energy dissipation due to re-bending will be minor.

STRETCHING CONTRIBUTION

The main part of the energy, during the local penetration is dissipated in the stretching of the stiffened hull plating and girders. The local penetration can be broken into phases so that force deformation equations can be defined for each phase. As mentioned above, bending is estimated to contribute less than 8% of the total energy dissipated, and does not significantly change the length of the transition zone L. For the remainder of this analysis membrane energy will be de-coupled from bending energy to simplify calculations.

OUTER PLATE DEFORMATION ($n = 1$)

The outer plate is assumed to deform in a diamond shape as shown in Figure 4. Define α , β , and δ , as shown below.

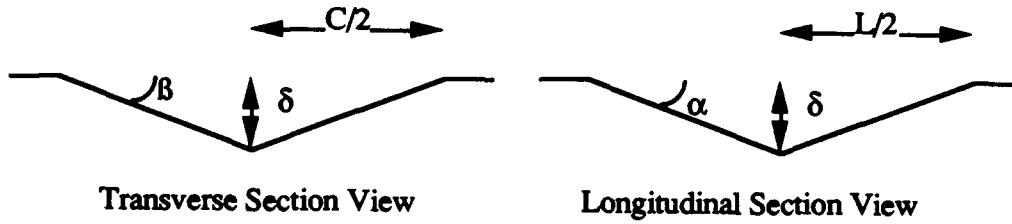


Figure 8 Diamond Shape Deformation of the Outer Plate

The rate of energy dissipation, due to the initial stretching of the outer plate, is calculated;

$$\dot{E}_m = \int_S N_o \dot{\epsilon}_1 ds + \int_S N_o \dot{\epsilon}_2 ds \quad (2)$$

where $\dot{\epsilon}_1 = \beta \dot{\beta}$ is the strain rate in the transverse direction, $\dot{\epsilon}_2 = \alpha \dot{\alpha}$ is the strain rate in the longitudinal direction, N_o is the plastic membrane force per unit width, and S is one quadrant of the area of deformed metal.

Using a small angle approximation, it can be shown that;

$$\dot{\epsilon}_1 = \left(\frac{\dot{\delta}}{C/2}\right)\left(\frac{\dot{\delta}}{C/2}\right) \quad (3a)$$

$$\dot{\epsilon}_2 = \left(\frac{\dot{\delta}}{L/2}\right)\left(\frac{\dot{\delta}}{L/2}\right) \quad (3b)$$

Therefore;

$$\dot{E}_m = \frac{C}{2} L N_o \dot{\epsilon}_1 + C \frac{L}{2} N_o \dot{\epsilon}_2 \quad (4)$$

$$\dot{E}_m = N_o \dot{\delta} \left[L \frac{\delta}{C/2} + C \frac{\delta}{L/2} \right] \quad (5)$$

The force deformation relation can be found by setting the external rate of work equal to the internal rate of energy dissipation;

$$\dot{E}_{ext} = P\dot{\delta} \quad (6)$$

$$P\dot{\delta} = N_o\dot{\delta}\left[L\frac{\dot{\delta}}{C/2} + C\frac{\dot{\delta}}{L/2}\right] \quad (7)$$

$$P = \left[LN_o\frac{\dot{\delta}}{C/2} + CN_o\frac{\dot{\delta}}{L/2}\right] \quad (8)$$

It can be postulated that for any given penetration depth δ , the distance L adjusted itself so that P is minimized.

$$\frac{\partial P}{\partial L} = N_o\frac{\dot{\delta}}{C/2} - 2CN_o\dot{\delta}L^{-2} \quad (9)$$

from which;

$$L_1 = C \quad (10)$$

In Appendix B, with bending included, L is determined to be;

$$L = \frac{1}{\sqrt{\frac{4M_o + N_o\delta}{N_o C^2 \delta}}} \quad (B.15)$$

Equation (B.16) reduces to Equation (10) for $M_o = 0$

It is possible to check the above approximation for specific examples. In Appendix C, L is calculated using equation (B.16) for a stiffened plate and a simple plate. The results show;

$$L(\text{stiffened plate}) = 0.92 C \quad (\text{C.1})$$

$$L(\text{simple plate}) = 0.99 C \quad (\text{C.2})$$

This indicates that a reasonably small error is incurred with this approximation.

Using this result in equation (5), and accounting for all 4 quadrants of the area the rate of energy dissipation due to stretching the outer plate becomes;

$$\dot{E}_m = \delta(4N_o\dot{\delta}) \quad (11)$$

This result will apply until the outer plate ruptures or the first set of girders is reached by the reef. Rupture is assumed to occur at a strain of 10%, for commercial shipbuilding steel⁵;

$$\epsilon_{cr} = 0.1 \quad (12)$$

Assuming triangular deformation as shown in Figure 8, the displacement function is;

$$w(y) = \delta(1 - \frac{2y}{C}) \quad (13)$$

⁵McDermott, J.F., Kline, R.G., Jones, E.L. Maniar, N.M., and Chiang, W.P., "Tanker Structural Analysis for Minor Collisions", Transaction of the Society of Naval Architects and Marine Engineers, Vol.82, pp229-414

' δ ' critical is calculated;

$$\delta_{cr} = C \sqrt{\frac{E_{cr}}{2}} \quad (14)$$

$$\delta_{cr} = 0.22C \quad (15)$$

Therefore, the plate will rupture before the first set of longitudinal girders is reached, as long as β of the reef is of at least a minimum angle:

$$\tan \beta = \delta_{cr} / C \quad (16)$$

$$\beta_{cr} = 0.42 \text{ rad} \quad (17)$$

If β is less than this value, rupture of the outer plate due to membrane strain will never occur since the hinge position will continue to move to each successive set of girders before $\beta_{cr} = 0.42 \text{ rad}$ is reached.

DEFORMATION OF 3 CELLS ($n = 3$)

Once the first set of girders are reached by the reef the girders must be deformed, and a second set of hinges in the outer plate form as shown below.

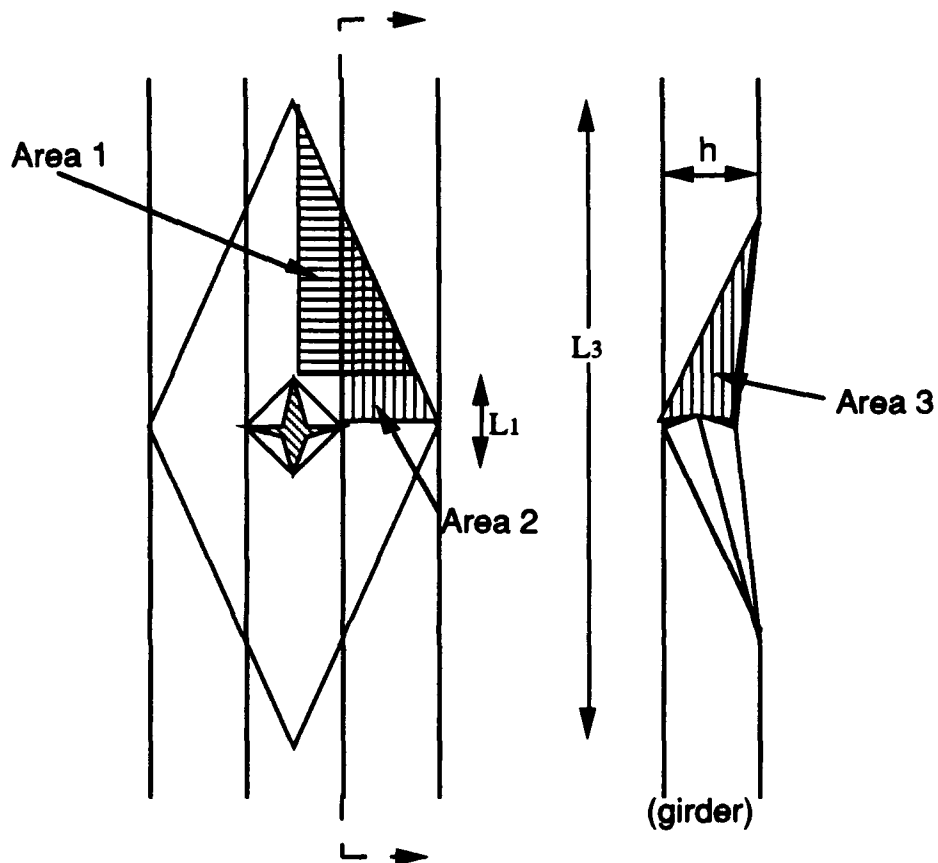


Figure 9 - Membrane Stretching Over Three Cells

The rate of energy dissipation, due to the stretching of the three areas shown, is calculated;

$$\dot{E}_m = 4 \left[\int_{A_1} N_o \dot{\epsilon}_1 dS_{A_1} + \int_{A_2} N_o \dot{\epsilon}_2 dS_{A_2} + \int_{A_3} N_o \dot{\epsilon}_2 dS_{A_3} \right] \quad (18)$$

These areas and strain rates can be shown by geometry to be;

$$A_1 = \frac{(L_3 - L_1)^2 (3C)}{L_3^2} \quad (19a)$$

$$\dot{\epsilon}_1 = \beta \dot{\beta} \equiv \frac{\delta \dot{\delta}}{\left[\frac{3C}{2} \left(\frac{L_3 - L_1}{L_3} \right) \right]^2} \quad (20a)$$

$$A_2 = \frac{1}{2} \left(\frac{L_3}{3} \right) (C) \quad (19b)$$

$$\dot{\epsilon}_2 \equiv \alpha \dot{\alpha} = \frac{9\delta \dot{\delta}}{L_3^2} \quad (20b)$$

$$A_3 = \frac{1}{2} \left(\frac{L_3}{3} \right) (h) \quad (19c)$$

$$\dot{\epsilon}_2 \equiv \alpha \dot{\alpha} = \frac{9\delta \dot{\delta}}{L_3^2} \quad (20c)$$

Therefore;

$$\dot{E}_m = 4N_o \delta \dot{\delta} \left[\left(\frac{L_3}{6C} \right) + \left(\frac{3C}{2L_3} \right) + \left(\frac{3h}{2L_3} \right) \right] \quad (21)$$

Minimizing the energy dissipation with respect to L , yields L_3 in terms of C , h ..

$$\frac{dP}{dL_3} = 2N_o \delta \left[\frac{1}{3C} - (3C + 3h)L_3^{-2} \right] = 0 \quad (22)$$

$$L_3 = 9(C^2 + Ch)^{1/2} \quad (23)$$

Using the same rupture criteria, a second rupture of the outer plate, and rupture of the first girders, will occur when;

$$w(y) = \delta(1 - \frac{2y}{3C}) \quad (24)$$

$$\delta_{cr} = 0.67C \quad (25)$$

This second rupture will occur if β of the reef is of at least a minimum angle;

$$\tan \beta = \delta(\frac{2}{3C}) \quad (26)$$

$$\beta_{cr} = 0.42 \text{ rad} \quad (27)$$

This is the same critical angle as the first rupture. This critical rupture angle is a constant indicating that the outer plate will rupture in a step fashion starting with the first cell, if at all.

DEFORMATION OF 5 CELLS ($n = 5$)

Membrane Energy over 5 cells can be derived in a similar manner:

$$E_m = 4N_o\delta\delta[(\frac{L_5}{10C}) + (\frac{5C}{2L_5}) + (\frac{5h}{2L_5})] \quad (28)$$

$$L_5 = 25(C^2 + Ch)^{1/2} \quad (29)$$

$$\delta_{cr} = 1.12C \quad (30)$$

DEFORMATION OF 'n' CELLS

A general expression for membrane energy over "n" cells, where "n" is an odd integer, can be derived. The result is as follows;

$$E_{m_n} = 2N_o\delta\delta\left[\frac{L_n}{nC} + \frac{nC}{L_n} + \frac{nh}{L_n}\right] \quad (31)$$

$$L_n = n^2(C^2 + Ch)^{1/2} \quad (32)$$

$$\delta_{cr} = 0.224nC \quad (33)$$

These results apply until the reef reaches the inner plate, when $\delta = h$.

DEFORMATION OF THE INNER PLATE

The contribution to membrane energy from the inner plate can be derived in an identical fashion as equations (10) and (11) for the outer plate. This results as follows:

$$E_{m_i} = 2N_o\delta\delta\left[\frac{L_i}{nC} + \frac{nC}{L_i}\right] \quad (34)$$

$$L_i = nC \quad (35)$$

Without loss of generality,

$$E_{m_i} = 4N_o\delta\delta \quad (36)$$

The total membrane energy after the reef reaches the inner plate, and before rupture, is;

$$E_m = E_{m_i} + E_{m_n}$$

This result applies until the inner plate ruptures.

RUPTURE OF THE INNER PLATE

Given the geometry of the cell and again assuming a triangular deformation profile, the critical penetration distance for rupture of the inner plate can be calculated as follows;

$$w(y) = \delta_{op}(1 - \frac{2y}{nC}) \quad (37)$$

$$\delta_{opcr} = nC \sqrt{\frac{\epsilon_{cr}}{2}} \quad (38)$$

$$\delta_{opcr} = 0.224nC \quad (39)$$

where δ_{opcr} is the additional penetration distance after contacting the inner plate.

This indicates that the minimum reef angle, β , that will cause rupture of the inner plate can be calculated as;

$$\tan\beta = (0.224nC + h) \frac{2}{nC} \quad (40)$$

So for a square cell, the inner plate will rupture over either 1 or 3 cells;

$$\text{for } h = C, \quad n=1 \quad \beta_{cr} = 1.18 \text{ rad} \quad (41)$$

$$n=2 \quad \beta_{cr} = 0.84 \text{ rad} \quad (42)$$

$$(n=5 \quad \beta_{cr} = 0.955 \text{ rad}) \quad (43)$$

it is concluded that;

Very steep reef (top angle of reef < 44 degrees) will rupture over 1 cell.

Moderately steep reef (44 < angle < 84 degrees) will rupture over 3 cells.

Gradually sloped reef (top angle > 84 degrees) will not rupture the inner plate.

The duration of each of the above phases depends on the transverse angle of the reef β , and the relative height, h , and width, c , of the cells. The resulting membrane force-deformation functions for a square cell hull structure are shown in Figure 10.

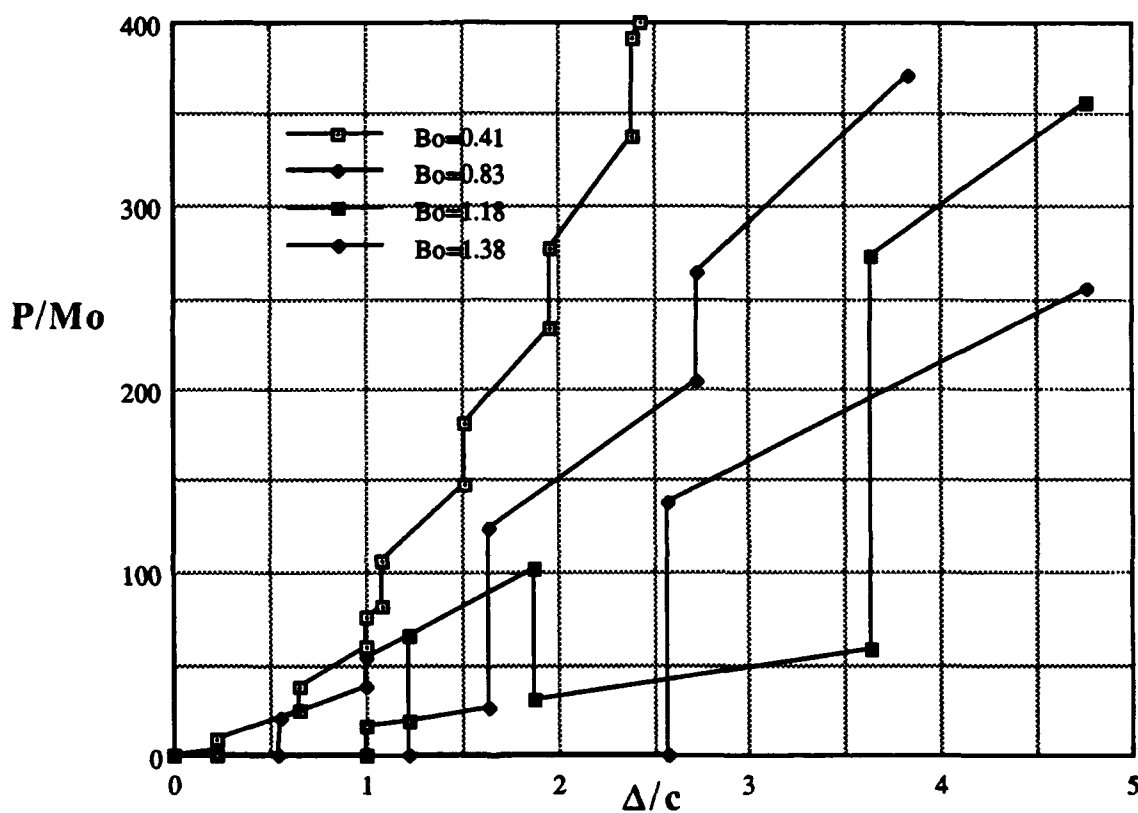


Figure 10 - Membrane Force vs Penetration Depth for Square Cell Structure

TOTAL FORCE DEFORMATION RELATIONSHIP

The total energy dissipation and force deformation relationship for a specific hull structure can be estimated by adding the bending and stretching components. A bending contribution can be calculated for a given plate thickness, stiffener size, and spacing, as shown in Appendix C. The stretching contribution can be calculated for a given C , h , and N_o as shown above. The total energy dissipation can be calculated by summing these two components. These calculations were completed for a DTRC design of a 39,000 dwt USDH tanker and are included in Appendix D. Figures 11 - 14 show the estimated force-deformation relationship for a range of reef angles.

Figure 11 shows the force - deformation relationship for a USDH and a reef with a small (gradual) spreading angle. There is a steady step like increase in force with increasing penetration as each additional set of cells is reached. There is an additional step increase at $\Delta/C = 1$ when the inner plate is reached. No rupture occurs.

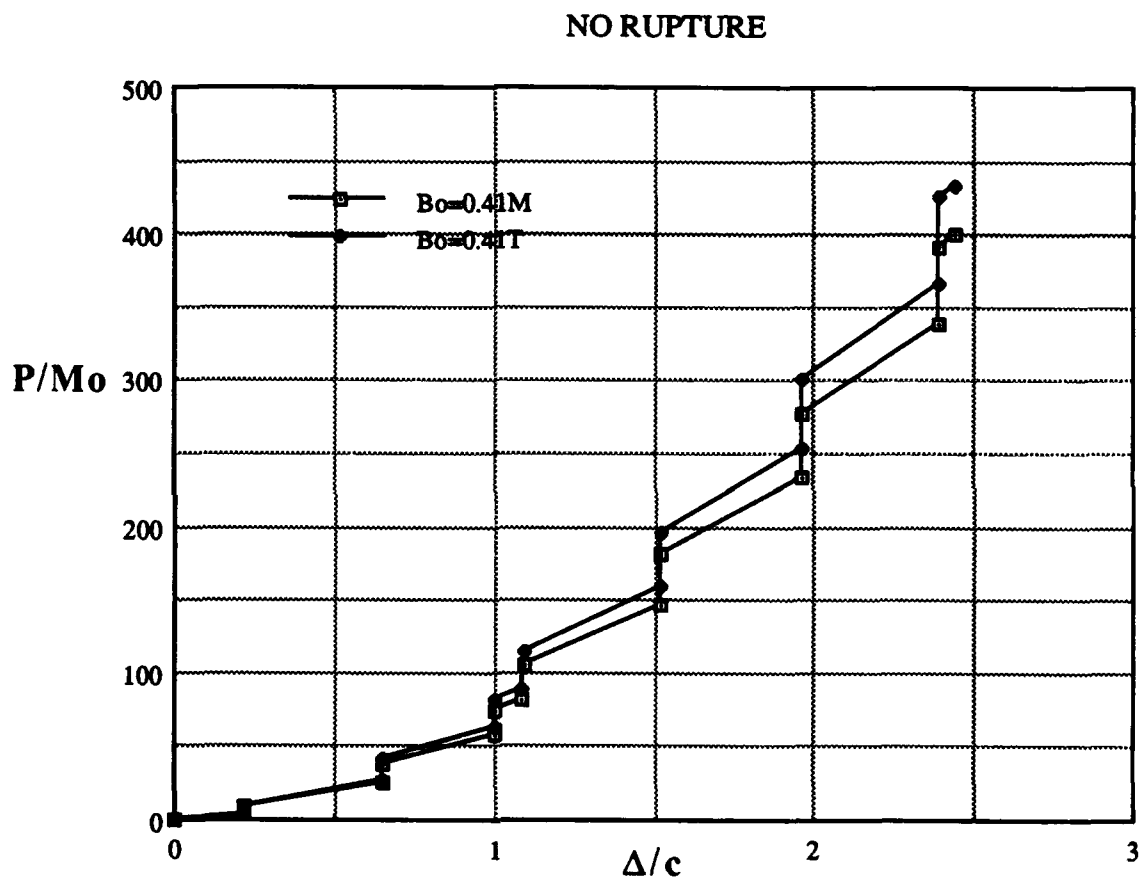


Figure 11 - Force-Deformation Relationship for $Bo = 0.41$

Figure 12 shows the force - deformation relationship for a USDH and a reef with a moderate spreading angle. A sudden loss of strength is noted with the outer plate ruptures and again when a second rupture of the outer plate and the first set of girders occurs. This pattern of step increases and sudden losses of strength will continue as each set of girders is reached and ruptures.

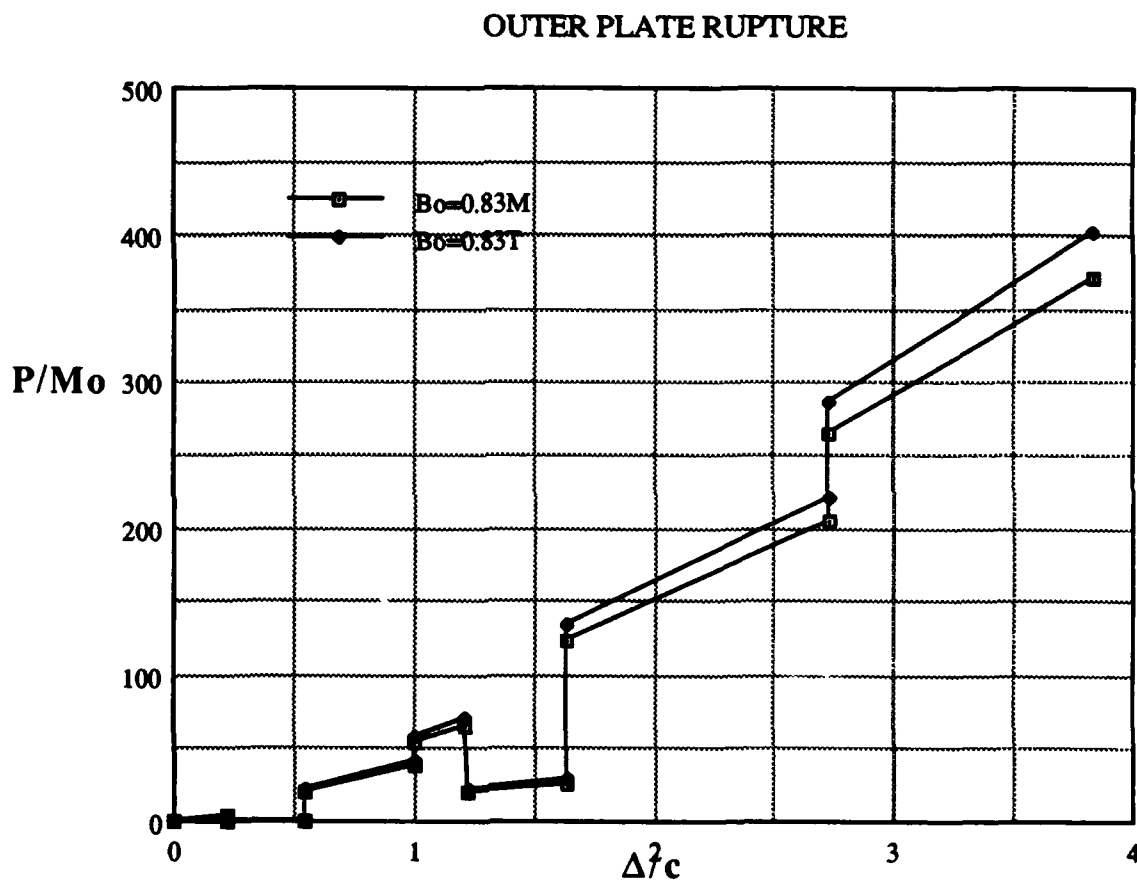


Figure 12 - Force-Deformation Relationship for $Bo = 0.83$

Figure 13 shows the force - deformation relationship for a USDH and a reef with a steep spreading angle. The force increases slightly with outer plate deformation, there is a loss of strength with outer plate rupture, the force has a step increase when the inner plate is reached ($\Delta/C = 1$), steadily increases, has a second step increase when the first set of girders is reached, steadily increases, and has a large loss of strength when the inner plate ruptures coincidentally with the second outer plate and girder rupture. Strength is regained and continues to increase when the second set of girders is reached and the pattern continues.

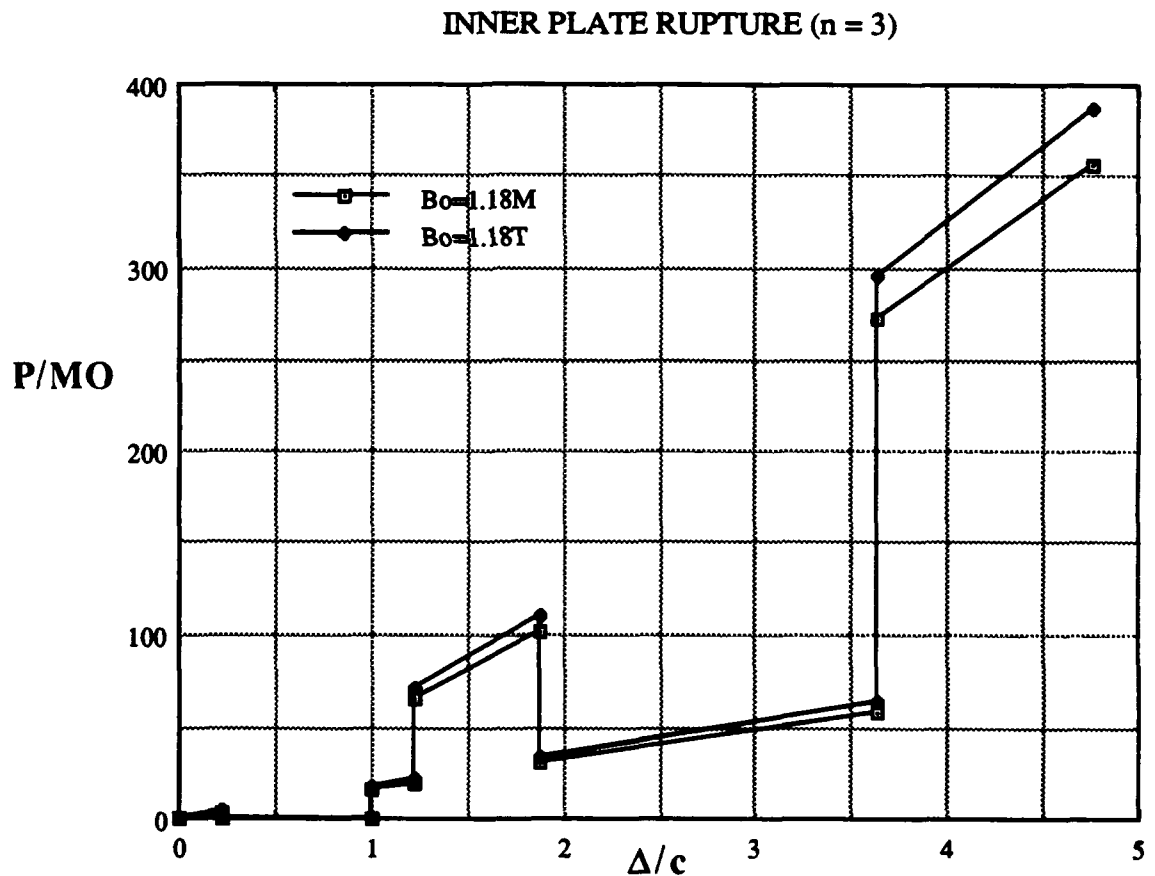


Figure 13 - Force Deformation Relationship for $Bo = 1.18$

Figure 14 shows the force - deformation relationship for a USDH and a reef with a very steep spreading angle. The force increases slightly with outer plate deformation, there is a loss of strength with outer plate rupture, the force has a step increase when the inner plate is reached, there is a second loss of strength when the inner plate ruptures, and a large step increase when the first set of girders are reached and consequently new regions of the outer and inner plate become active.

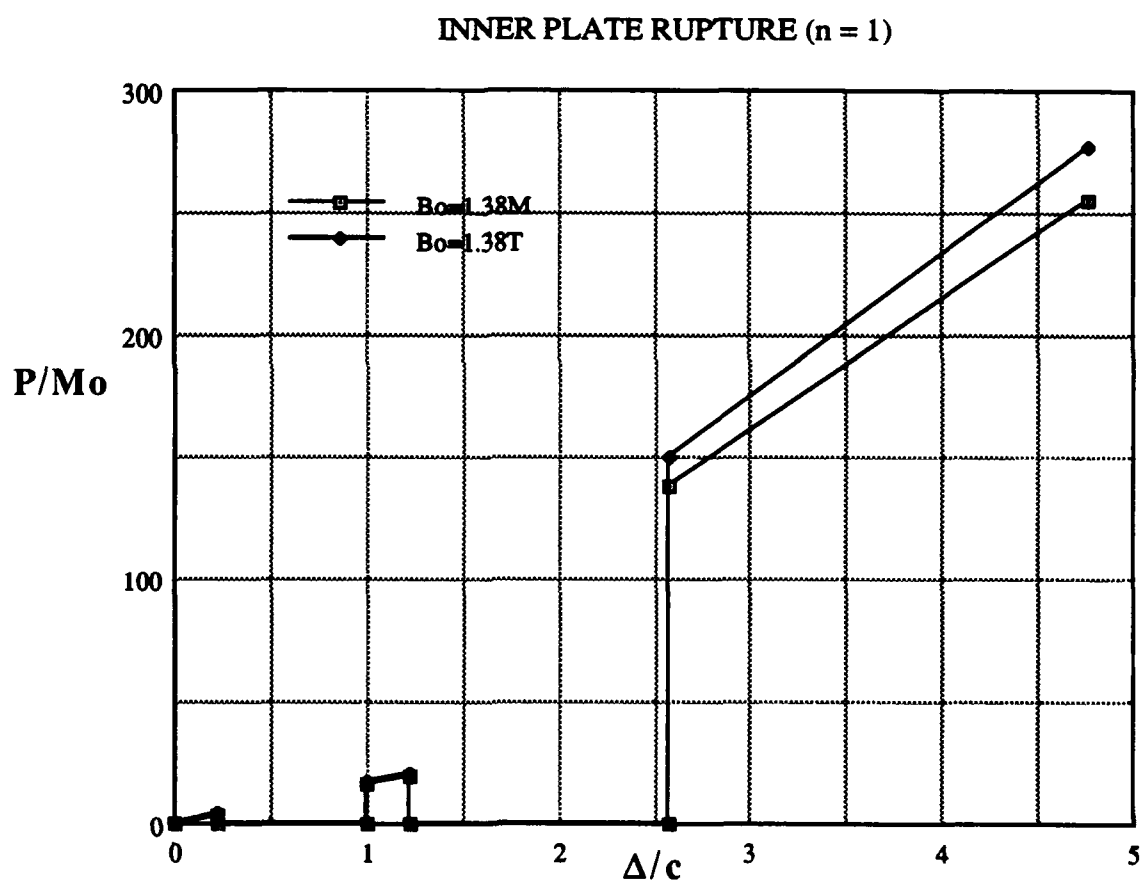


Figure 14 - Force-Deformation Relationship for $Bo = 1.38$

FORCE BALANCE

RELATIVE DISTRIBUTION OF LIFT AND PENETRATION

As described in the formulation of the problem, three relationships must be solved simultaneously in order to determine the penetration depth Δ ; the expression for the reaction force - equation (1), the force of deformation functions graphed in Appendix D, and the geometry constraint $\Delta_R = \Delta + \Delta_1$. The simultaneous solution of these three equations, for varying reef angle β , can be represented graphically. Appendix E shows the data required to graphically represent the simultaneous solution of these three equations for the DTRC USDH tanker. Reaction force, R , and force of deformation, P , both normalized with plastic bending moment, M_0 , are plotted against penetration distance, Δ , normalized by cell width, C . The height of the reef, Δ_R , is the sum of these two distances. Δ_R is represented in Figure 15 as the distance between a lift function R/M_0 , and a penetration function P/M_0 . Therefore, for a given reef height the corresponding lift and penetration distance can be found.

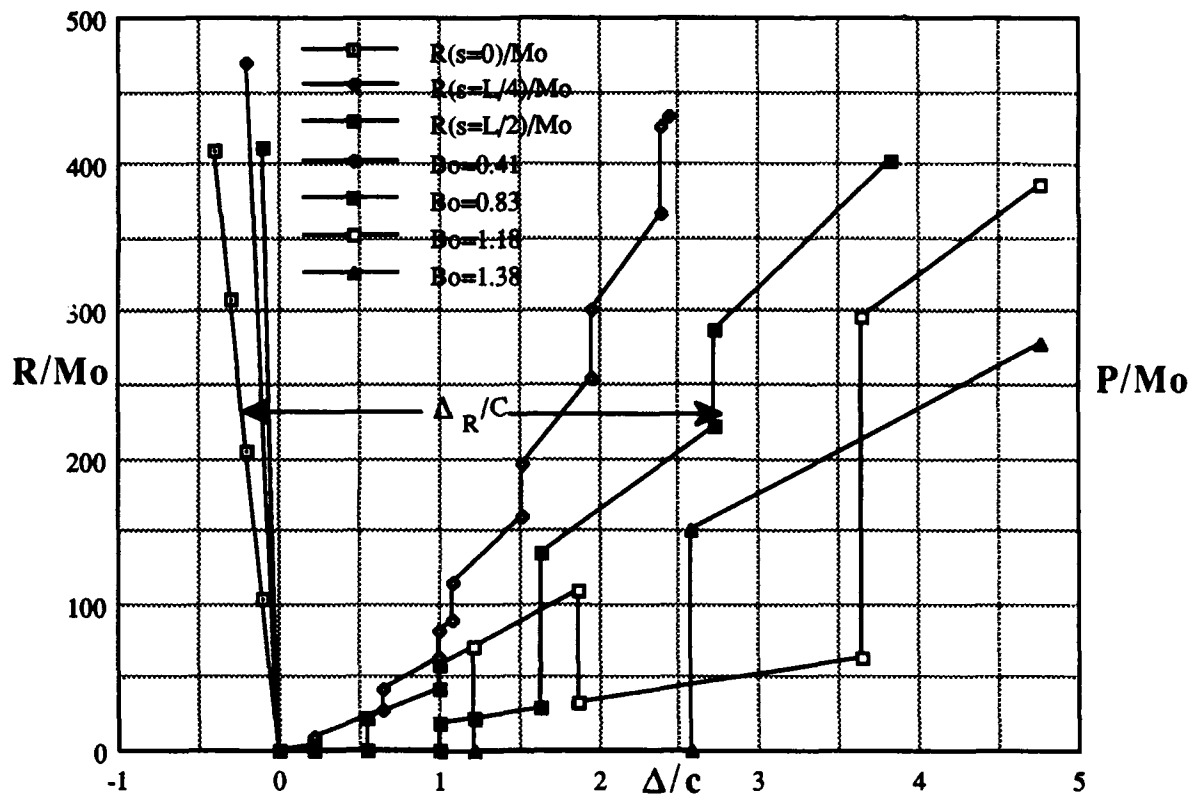


Figure 15 - Relative Distribution of Lift and Penetration

RESULTS AND DISCUSSION

By applying the energy balance method developed by Wierzbicki et al.⁶ for single hull ships; force-deformation relationships for Unidirectionally Stiffened Double Hulls during the initiation of local damage have been developed. No restrictions have been placed of the gross characteristics of the vessel, other than a flat bottom in the area of the damage. The height and width of the structural cells are allowed to vary independently, as well as the degree of plate stiffening. The height and spreading angle of the reef are allowed to vary as well. Four major assumptions were made. The initiation phase was idealized as being purely vertical damage. The energy dissipation due to fracture was neglected. The bending/membrane energy ratio for a given structure was assumed to remain constant with increasing penetration. And a rupture criterion of $\epsilon_{cr} = 0.1$ is assumed.

These assumptions allowed the derivation of force-deformation functions which determine length of transition zone L , lateral extent of damage nC , and vertical resisting force P , as a function of penetration distance Δ , reef spreading angle β , and cell geometry. These functions combined with a function for the reaction force on the ship R , and the height of the reef Δ_R are used to derive a penetration distance Δ and an amount of lift Δ_l for a given grounding.

⁶Wierzbicki, T. et al.

The functions can also be used to derive critical reef angles β that will cause rupture. These angles are illustrated in Figure 16 for a square cell geometry.

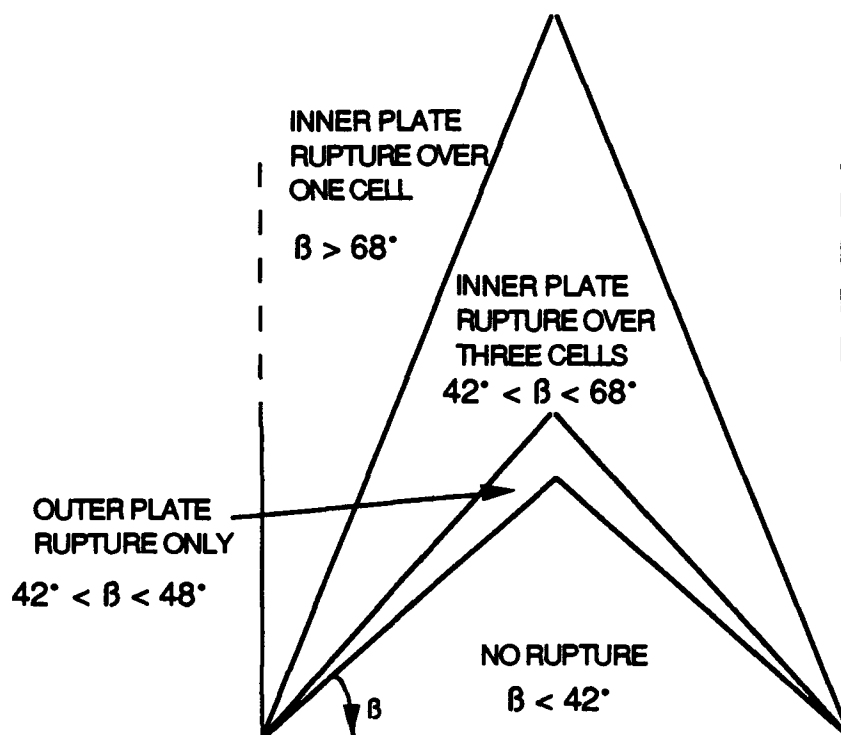


Figure 16 Critical Reef Angles β that will Cause Rupture for a square cell.

Critical reef heights for a given ship can also be calculated as a function of spreading angle.

CONCLUSIONS AND RECOMMENDATIONS

This paper develops analytical tools needed to compare different hull structure designs and their merits for withstanding grounding damage. The extent of hull penetration has been calculated and related to the ships gross characteristics, hull structure geometry, and the geometry of the obstruction. The extent of hull penetration and lifting for varying reef heights and spreading angles for a square celled USDH tanker are given as an example. Such a model can be a valuable tool in developing ship designs and in writing realistic regulations for the shipping industry. Required critical reef heights and spreading angles for inner hull rupture can be defined for different classes of ships. Regulations based on critical reef dimensions would be more directly related to the probability of oil outflow than regulations based on double bottom height. Design trade off studies can be conducted based on predicted critical reef heights for different design options. It can be shown that for a given structure if the height to width ratio of the cells is increased the critical reef spreading angle is also increased. However, If the height of the cells is increased the cargo capacity is reduced, or the stability is degraded. If the width of the cells is decreased the weight of the structure is increased. Cell height, width, and degree of stiffening can be varied so as to achieve a maximum critical reef height for a given structural weight or total cost.

In Reference 6, by Yukio Ueda et al., an ultimate strength analysis of a traditional box type double bottom structure in a stranding condition is analysed. A cylindrical stranding rock, with no spreading, is assumed. The resulting force deformation curves show stepped functions similar to those derived in this paper. Model test are needed to confirm the theoretical results derived in this paper. Further work is also required to relax the assumptions made in this paper, specifically the energy dissipated in fracture and re-bending should be estimated. The corresponding functions for the steady state grounding phase need to be derived so that the longitudinal extent of damage can be predicted.

REFERENCES

1. Okamoto, Tomiyasu et al, "Strength Evaluation of Novel Unidirectional-Girder-System Product Oil Carrier by Reliability Analysis" Trans. SNAME, Vol93,1985.
2. Beach, J. "Cluster Technologies," Trans. ASNE Destroyer, Cruiser, and Frigate Symp. 29 Sept. 1990
3. Hughes, Owen F. "Ship Structural Design, A Rationally - Based, Computer - Aided Optimization Approach," SNAME, Jersey City, New Jersey.1988
4. Wierzbicki, T., Rady, E., Peer, D., and Shin, J.G., "Damage Estimates in High Energy Grounding of Ships", Joint M.I.T. Industry Program in Safe Tankers, Report No.1, June 1990
5. McDermott, J.F., Kline, R.G., Jones, E.L. Maniar, N.M., and Chiang, W.P., "Tanker Structural Analysis for Minor Collisions", Transaction of the Society of Naval Architects and Marine Engineers, Vol.82, pp 229-414
6. Ueda, Yukio., et al. "Ultimate Strength Analysis of Double Bottom Structures in Stranding Conditions", PRADS'87 Symposium. The Norwegian Institute of Technology, Norway, June 1987
7. Okumoto, Y., "Stranding and Ship Strength", Bulletin of the Society of Naval Architects of Japan, Vol.578 1977, pp. 7-15

APPENDIX A. FABRICATION OF USDH

This appendix addresses some of the welding difficulties associated with the geometry of Unidirectionally Stiffened Double Hulls (USDH) and some of the potential solutions. A brief explanation of this geometry and its producibility benefits are followed by possible near and mid term solutions available to the U.S. maritime industry.

GEOMETRY

Conventional mixed frame double hull structures are common for a wide range of liquid and dry bulk carriers. The inner and outer hulls are supported by an intersecting grillage of longitudinal stiffeners and transverse frames. Although this type of structure is producible by manual welding, it is unsuitable for automated welding due to the short welding runs required and frequent intersections of stiffening members. A USDH structure consist of longitudinal girders only joining the inner and outer hulls, forming a series of long cells. These girders are of common sizes, thicknesses, and material within the hull. This allows for continuous welds, potentially as long as each hull module.

NEAR TERM SOLUTIONS

The minimal access for welding personnel is considered to be about 3'x3'. Smaller USDH ship structures could approach this limit inside the cells. Internal continuous fillet welds along square butts are required to complete these cells. Manual welding in this application could be facilitated by a dolly system which would pull the welders along as they welded. Reducing the required number of passes, and proper ventilation, would be important. One possible assembly sequence could be as follows:

1. Down hand weld the fillet welds joining the girders to the inner plate, leaving a section of inner plate off at the ends of the module (Girders would be staggered at the ends).
2. Complete all cut-outs, backing plates, grinding, etc on the inner plate.
3. Flip the inner plate and girder assembly onto the outer hull.
4. Down hand weld the girders to the outer hull.
5. Crane the module into position and mate it up with the neighboring module, weld the modules together through the access provided by the end sections of inner plate which are not yet in place.
6. Weld on the remaining sections of inner plate.

Hitachi Zonsen Corporation is using locally tended machines to complete these down hand welds in the building of four 40,000 dwt USDH tankers. Representatives from the U.S. Navy and private industry have traveled to Japan to observe their fabrication techniques. It was observed that extensive automation was not being used in the joining of the double hull structure. It appeared as if the curved sections of the hull were being assembled by down hand welding the girders to the outer shell using gravity feed welding machines on dollies, with tactile corner followers, tended by an operator. Each operator was tending about six machines by placing ~2 foot welding rods into them and manually

striking arcs. It is noted that the sections were not flipped to allow down-hand welding as might be expected. This may be due to the difficulty of handling large sections.

MID TERM SOLUTIONS

An automated welding process would work in an analogous manner with a tractor mounted welder performing gravity welds. An Independent Research and Development project conducted a research group at Ingalls, is developing a feasibility design for a machine to weld USDH structures. They are proposing a crawler-tractor with umbilicals back to a monitor/controller. The crawler would have a 4 or 5 degree of freedom torch manipulator, a video camera mounted on gimbals, and a laser system for tracking along the plate joints. Flux core welding is anticipated for lighter plating, and pulse MIG for heavier plating. A similar crawler could also be used for down hand finishing and for applying shell coatings. It is estimated, by a proponent, that this type of crawler could be ready for ship production as early as 1996 if sufficient research and development resources are allocated toward its development.

CONCLUSION

At present, the U.S. maritime industry can manually weld USDH structures with special attention being paid to the ventilation requirements of welding in confined spaces. A gravity feed welding machine, dolly mounted, with tactile corner followers, which would be manually tended, could be designed and ready for use within a year. This sort of machine would reduce the man hours required for these fillet welds by about a factor of five. If a similar welding machine could be designed with a continuous feed system it could take advantage of the long uninterrupted welds provided by a USDH design, and allow the tender to remain outside the cell during the final welds. A crawler-tractor type welder could greatly enhance productivity but requires a devoted R&D effort to be available for shipyard use in about 5 years.

APPENDIX B. BENDING - MEMBRANE SOLUTION FOR INDENTATION

1. Calculation of the rate of energy dissipation due to bending of outer plate. Define δ and β as shown below.

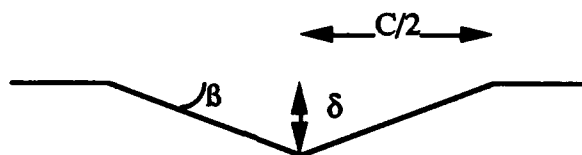


Figure B.1

Transverse Section View

Approximate the hinge length to the length of the transition zone, L . Energy dissipation due to bending can be calculated as follows;

$$\dot{E}_b = M_o(\dot{\beta} 4L) \quad (B.1)$$

where M_o is the fully plastic bending moment and $\dot{\delta} \equiv \dot{\beta} \frac{C}{2}$.

$$\dot{E}_b = 4M_o L \left(\frac{\dot{\delta}}{C/2} \right) \quad (B.2)$$

2. Calculation of the rate of energy dissipation due to stretching of outer plate (membrane energy). Define α as shown below.

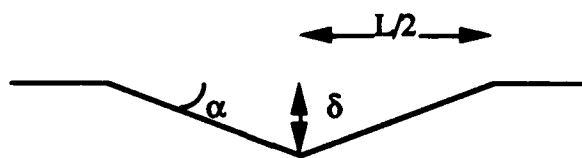


Figure B.2

Longitudinal Section View

$$\dot{E}_m = \int_S N_o \dot{\epsilon}_1 ds + \int_S N_o \dot{\epsilon}_2 ds \quad (B.3)$$

where N_o is the fully plastic membrane force per unit width.

$$\dot{\epsilon}_1 = \beta \dot{\beta} \quad (B.4a)$$

$$\dot{\epsilon}_2 = \alpha \dot{\alpha} \quad (B.4b)$$

Using a small angle approximation;

$$\dot{\epsilon}_1 = \left(\frac{\delta}{c/2}\right) \left(\frac{\dot{\delta}}{c/2}\right) \quad (B.5a)$$

$$\dot{\epsilon}_2 = \left(\frac{\delta}{L/2}\right) \left(\frac{\dot{\delta}}{L/2}\right) \quad (B.5b)$$

Substituting;

$$\dot{E}_m = \frac{c}{2} L N_o \dot{\epsilon}_1 + C \frac{L}{2} N_o \dot{\epsilon}_2 \quad (B.6)$$

$$\dot{E}_m = N_o \dot{\delta} \left[L \frac{\delta}{c/2} + C \frac{\delta}{L/2} \right] \quad (B.7)$$

3. Total rate of energy dissipation.

$$\dot{E}_T = \dot{E}_b + \dot{E}_m \quad (B.8)$$

$$\dot{E}_T = \dot{\delta} \left[4M_o L \frac{1}{C/2} + N_o L \frac{\delta}{C/2} + N_o C \frac{\delta}{L/2} \right] \quad (B.9)$$

Energy balance

$$\dot{E}_{ext} = P \dot{\delta} \quad (B.10)$$

therefore ;

$$P = \left[\frac{4M_o}{C/2} + \frac{N_o \delta}{C/2} \right] L + \frac{2N_o C \delta}{L} \quad (B.11)$$

where P is the vertical resisting force.

4. Minimize the energy with respect to L, so as to determine the relation between L and C.

$$\frac{dP}{dL} = 0 \quad (B.12)$$

$$P = AL + \frac{B}{L} \quad (B.13)$$

$$L = \frac{1}{\sqrt{\frac{A}{B}}} \quad (B.14)$$

$$L = \frac{1}{\sqrt{\frac{4M_o + N_o\delta}{N_o C^2 \delta}}} \quad (B.15)$$

APPENDIX C. BENDING CONTRIBUTION

The percent of energy dissipation due to bending is calculated, during the initial outer plate deformation for a stiffened plate, and a simple plate of equivalent thickness;

1. Using the stiffened plate shown in Figure C.1, L is calculated.

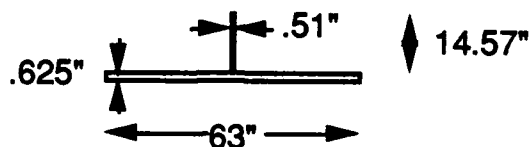


Figure C.1

Stiffened Plate

a. $A = 46.83 \text{ in}^2$ $I = 493 \text{ in}^4$ $C = 63 \text{ in}$
 $M_0 = 0.86 \sigma$ $N_0 = 0.74 \sigma$

Inserting these value into (B.16);

$$L = \frac{1}{\sqrt{\frac{4M_0 + N_0\delta}{N_0C^2\delta}}} \quad (\text{B.15})$$

$$L = 0.92 C \quad (\text{C.1})$$

b. Using a simple plate of equivalent thickness,

$A = 46.83 \text{ in}^2$ $I = 2.16 \text{ in}^4$ $C = 63$
 $M_0 = 0.14 \sigma$ $N_0 = 0.74 \sigma$

Inserting these value into (B.16);

$$L = 0.99 C \quad (\text{C.2})$$

2. Calculate percent contribution of bending

$$P = 4M_oL\left(\frac{1}{C/2}\right) + (N_oC\frac{\delta}{C/2} + N_oC\frac{\delta}{L/2}) \quad (B.11)$$

a. For stiffened plate,

$$\frac{P}{\sigma} = 6.32 + 74.27 \quad \text{in}^2$$

$$\frac{P}{\sigma} = 7.8\%(\text{Bending}) + 92.2\%(\text{Membrane}) \quad (C.3)$$

b. For simple plate

$$\frac{P}{\sigma} = 1.5\%(\text{Bending}) + 98.5\%(\text{Membrane}) \quad (C.4)$$

APPENDIX D. TOTAL FORCE DEFORMATION RELATIONSHIP

This appendix shows the calculation for the total force balance during the local penetration phase of grounding for the DTRC design for a 40,000 dwt USDH tanker. The force deformation relationship for membrane energy was derived in the STRETCHING CONTRIBUTION section. The bending contribution is assumed to be a constant 7.8% as derived in Appendix C.

$$\frac{P}{\sigma} = 7.8\%(\text{Bending}) + 92.2\%(\text{Membrane}) \quad (\text{C.3})$$

Therefore the total rate of energy dissipation is assumed to be;

$$\dot{E}_T = \dot{E}_m \left(\frac{1}{0.922} \right) \quad (\text{D.1})$$

Spread Sheet D calculates the normalized membrane and total force deformation relationship for given normalized penetration distances. Figures 11-14 were generated from this spreadsheet. They show the normalized membrane force, M, and total force, T, for the reef spreading angles $\beta = 0.41$ rad., $\beta = 0.83$ rad., $\beta = 1.18$ rad, and $\beta = 1.38$ rad., respectively.

SPREAD SHEET D								
Δ/c	B=0.41M	B=0.83M	B=1.18M	B=1.38M	B=0.41T	B=0.83T	B=1.18T	B=1.38T
0e+0	0e+0	0e+0	0e+0	0e+0	0e+0	0e+0	0e+0	0e+0
2.2e-1	3.52e+0	3.52e+0	3.52e+0	3.52e+0	3.817792e+0	3.817792e+0	3.817792e+0	3.817792e+0
2.21e-1	8.336e+0	0e+0	0e+0	0e+0	9.0412256e+0	0e+0	0e+0	0e+0
5.5e-1		0e+0				0e+0		
5.51e-1		2.0712e+1				2.24642352e+1		
6.5e-1	2.452e+1				2.6594392e+1			
6.51e-1	3.8304e+1				4.15445184e+1			
1e+0	5.884e+1	3.772e+1	0e+0	0e+0	6.3817864e+1	4.0911112e+1	0e+0	0e+0
1.001e+0	7.4916e+1	5.3772e+1	1.6016e+1	1.6016e+1	8.12538936e+1	5.83211112e+1	1.73709536e+1	1.73709536e+1
1.09e+0	8.1576e+1				8.84773296e+1			
1.091e+0	1.05608e+2				1.145424368e+2			
1.22e+0		6.554e+1	1.952e+1	1.952e+1		7.1084684e+1	2.1171392e+1	2.1171392e+1
1.221e+0		1.9536e+1	6.5556e+1	0e+0		2.11887456e+1	7.11020376e+1	0e+0
1.52e+0	1.47136e+2				1.595837056e+2			
1.521e+0	1.8112e+2				1.96442752e+2			
1.64e+0		2.624e+1				2.8459904e+1		
1.641e+0		1.22812e+2				1.332018952e+2		
1.88e+0			1.00992e+2				1.095359232e+2	
1.881e+0			3.0096e+1				3.26421216e+1	
1.96e+0	2.33396e+2				2.531413016e+2			
1.961e+0	2.77444e+2				3.009157624e+2			
2.39e+0	3.38136e+2				3.667423056e+2			
2.391e+0	3.92028e+2				4.251935688e+2			
2.439e+0	3.999e+2				4.3373154e+2			
2.57e+0				0e+0				0e+0
2.571e+0				1.38116e+2				1.498006136e+2
2.73e+0		2.04312e+2				2.215967952e+2		
2.731e+0		2.6436e+2				2.86724856e+2		
3.64e+0			5.824e+1				6.3167104e+1	
3.641e+0			2.72492e+2				2.955448232e+2	
3.83e+0		3.70744e+2				4.021089424e+2		
4.76e+0			3.5624e+2	2.55708e+2			3.86377904e+2	2.773408968e+2

APPENDIX E. FORCE BALANCE							
Δ/c	$R(s=0)/M_0$	$R(s=L/4)/M_0$	$R(s=L/2)/M_0$	$Bo=0.41$	$Bo=0.83$	$Bo=1.18$	$Bo=1.38$
0e+0				0e+0	0e+0	0e+0	0e+0
2.2e-1				3.817792e+0	3.817792e+0	3.817792e+0	3.817792e+0
2.21e-1				9.041225e+0	0e+0	0e+0	0e+0
5.5e-1					0e+0		
5.51e-1					2.24642352e+1		
6.5e-1				2.6594392e+1			
6.51e-1				4.15445184e+1			
1e+0				6.3817864e+1	4.0911112e+1	0e+0	0e+0
1.001e+0				8.12538936e+1	5.83211112e+1	1.73709536e+1	1.73709536e+1
1.09e+0				8.84773296e+1			
1.091e+0				1.145424368e+2			
1.22e+0					7.1084684e+1	2.1171392e+1	2.1171392e+1
1.221e+0					2.11887456e+1	7.11020376e+1	0e+0
1.52e+0				1.595837056e+2			
1.521e+0				1.96442752e+2			
1.64e+0					2.8459904e+1		
1.641e+0					1.332018952e+2		
1.88e+0						1.095359232e+2	
1.881e+0						3.26421216e+1	
1.96e+0				2.531413016e+2			
1.961e+0				3.009157624e+2			
2.39e+0				3.667423056e+2			
2.391e+0				4.251935688e+2			
2.439e+0				4.3373154e+2			
2.57e+0							0e+0
2.571e+0							1.498006136e+2
2.73e+0					2.215967952e+2		
2.731e+0					2.86724856e+2		
3.64e+0						6.3167104e+1	
3.641e+0						2.955448232e+2	
3.83e+0					4.021089424e+2		
4.76e+0						3.86377904e+2	2.773408968e+2
0e+0	0e+0	0e+0	0e+0				
-1e-1	1.02375e+2	2.3467e+2	4.1055e+2				
-2e-1	2.0475e+2	4.6935e+2					
-3e-1	3.07125e+2						
-4e-1	4.095e+2						